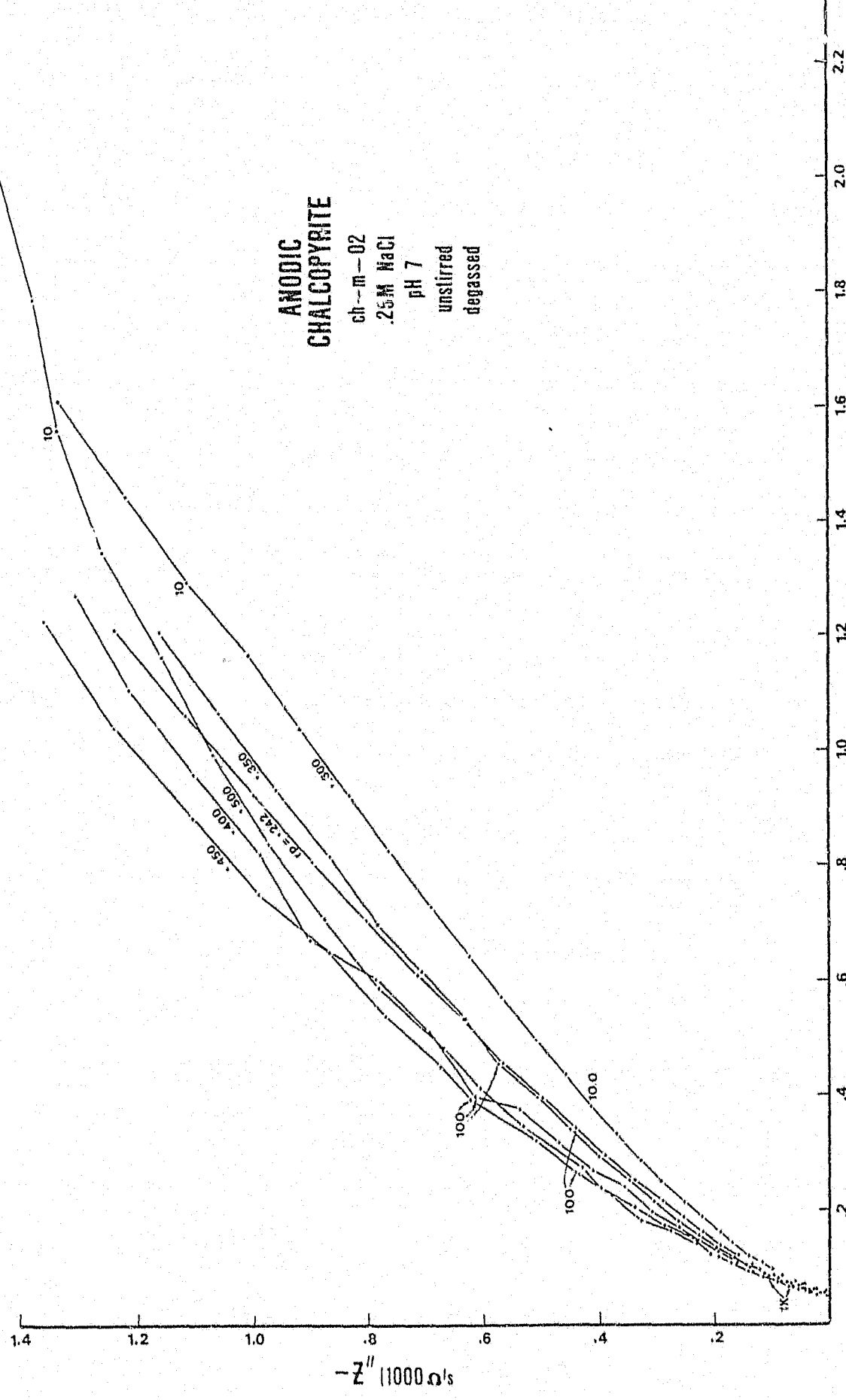

Fig. 4.22. Complex plane plot of the high frequency portion of the anodic impedance spectra for chalcopyrite shown in Fig. 4.21. (note scales).

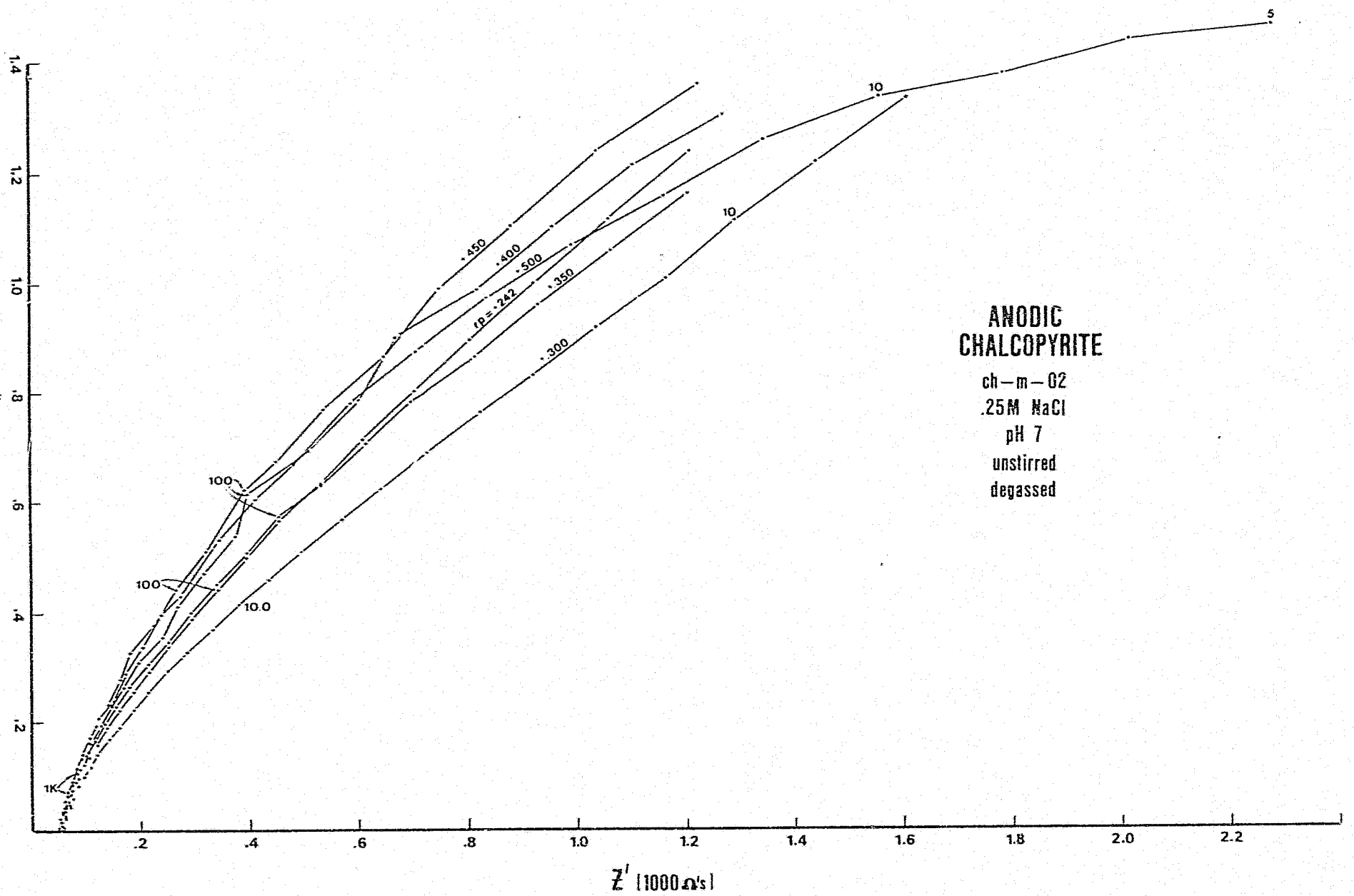

Fig. 4.22. Complex plane plot of the high frequency portion of the anodic impedance spectra for chalcopyrite shown in Fig. 4.21. (note scales).

the effects observed are due to solution phenomena. Alternatively, a surface or solid state diffusion phenomenon may be suggested.

As with pyrite, increasing the potential produces a corresponding decrease in impedance, as can be seen by the locus of the 0.1 Hz values. Very little change in impedance values for frequencies greater than 10 Hz is observed. Likewise for pyrite, although the locus of values is well ordered, the impedances do not change much in magnitude. Clearly then, in the frequency range from 10 Hz to 0.1 Hz, the differences in spectra between pyrite and chalcopyrite are significant.

4.6.2.2 Cathodic chalcopyrite

The spectra for various chalcopyrite electrodes measured at their rest potentials showed basically similar curve shapes to those of +242 mV and 0.0 mV. The only difference being a frequency striking along the +242 mV curve towards the 0.0 mV curve with decreasing rest potential. In the cathodic potential range of 0.0 to -200 mV very little change is observed in the spectra, presented in Fig. 4.23, either in curve shape or magnitude. Since the spectra are semicircular, a charge transfer reaction rate limiting process is indicated for all frequencies measured. This semicircle has a centre displaced well below the abscissa suggesting a dispersion of time constants for the rate limiting process. Amongst these processes could be solution Warburg impedance but stirring the solution while repeating the measurements, once again shows no effect. This suggests that the rate controlling reaction or process occurs in either the solid

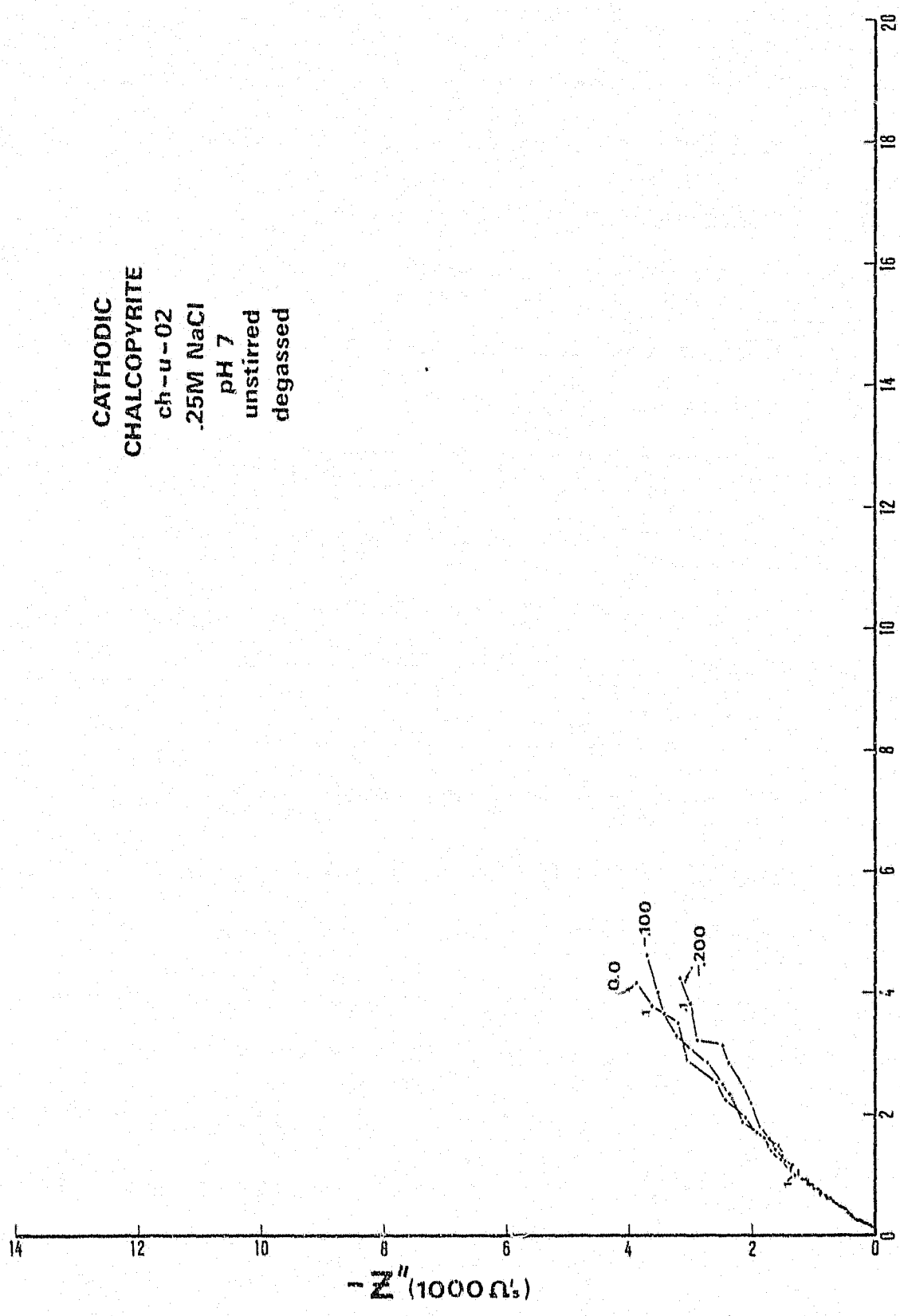

Fig. 4.23. Complex plane plot of cathodic impedance spectra for chalcopyrite.

state or surface. This corresponds to the observations made on anodic chalcopyrite.

4.6.2.3 Data from Angoran

Figs. 4.24 and 4.25 show the impedances measured by Angoran (1975) for chalcopyrite in two different supporting electrolytes. Note the abscissa and ordinate are normalized to the low frequency. An obvious disparity is evident between these data and those in Figs. 4.21 and 4.23 of this research in that no charge transfer is apparent in Fig. 4.24 and 4.25. This may be partially resolved by plotting a portion of a rest potential spectrum for ch-h-05 at an expanded scale as in Fig. 4.26. The spectrum for ch-h-05 does follow that of ch-m-02 quite closely at low frequencies. So a change in scale cannot totally resolve the apparent differences. However, the fundamental agreement is good enough to be able to say that the steep slopes observed by Angoran are not likely to be a result of solution Warburg impedance. Furthermore, impedance measurements performed while stirring the solution show no change at all, thus eliminating the possibility of solution diffusion control. The fitted equivalent circuit data of Angoran's are present with their respective plots. As with pyrite, the Warburg coefficient dominates the other parameters such that in an interpretation using only the computer fitted parameters one can too easily reach the conclusion that diffusion predominates.

4.6.3 Chalcopyrite and pyrite

Some trial impedance measurements combining chalcopyrite and pyrite electrodes in the same cell were performed. Very little difference from the chalcopyrite spectra was observed at rest potentials but with the addition of .01M $CuSO_4$ as

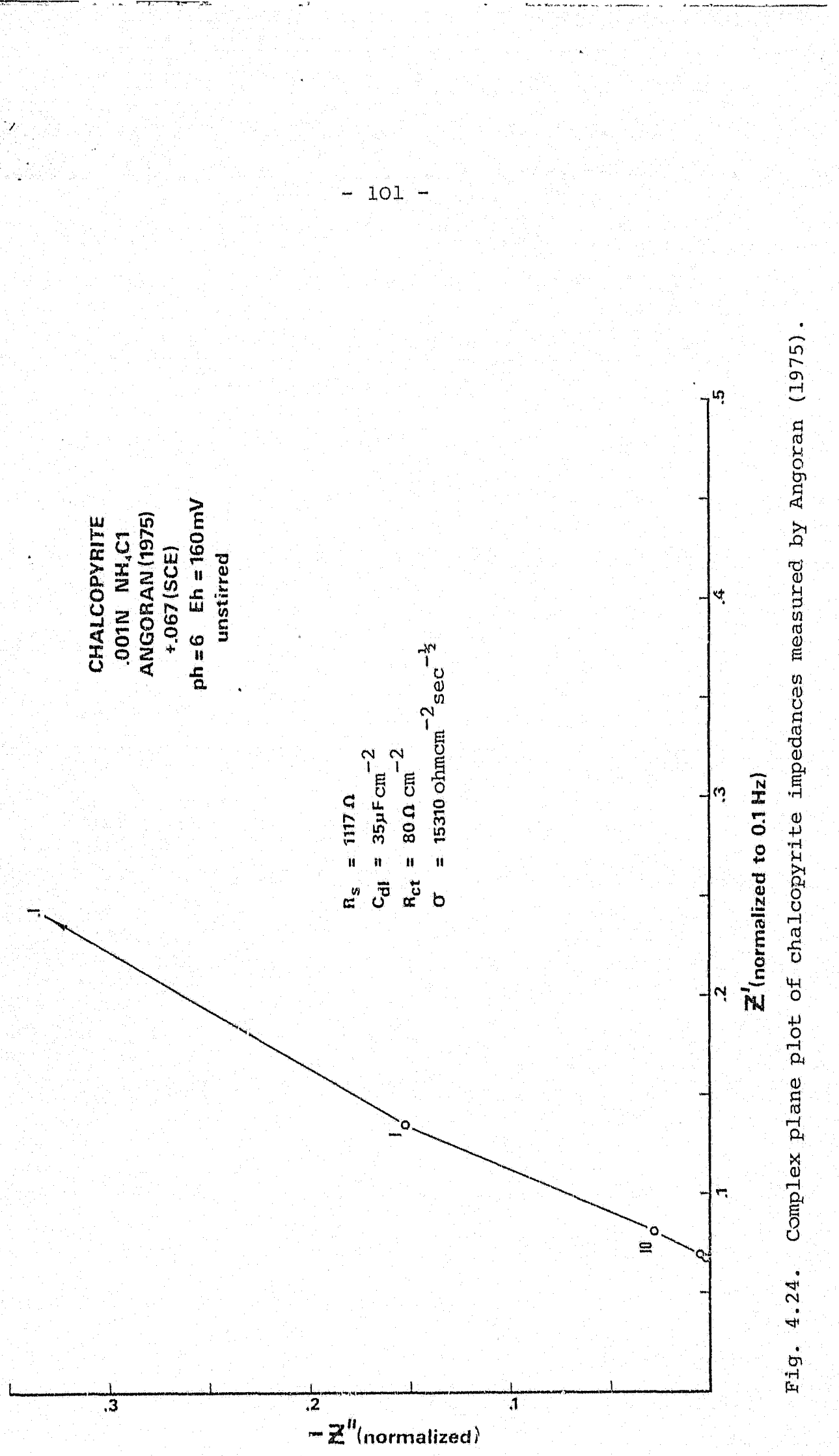

Fig. 4.24. Complex plane plot of chalcopyrite impedances measured by Angoran (1975).

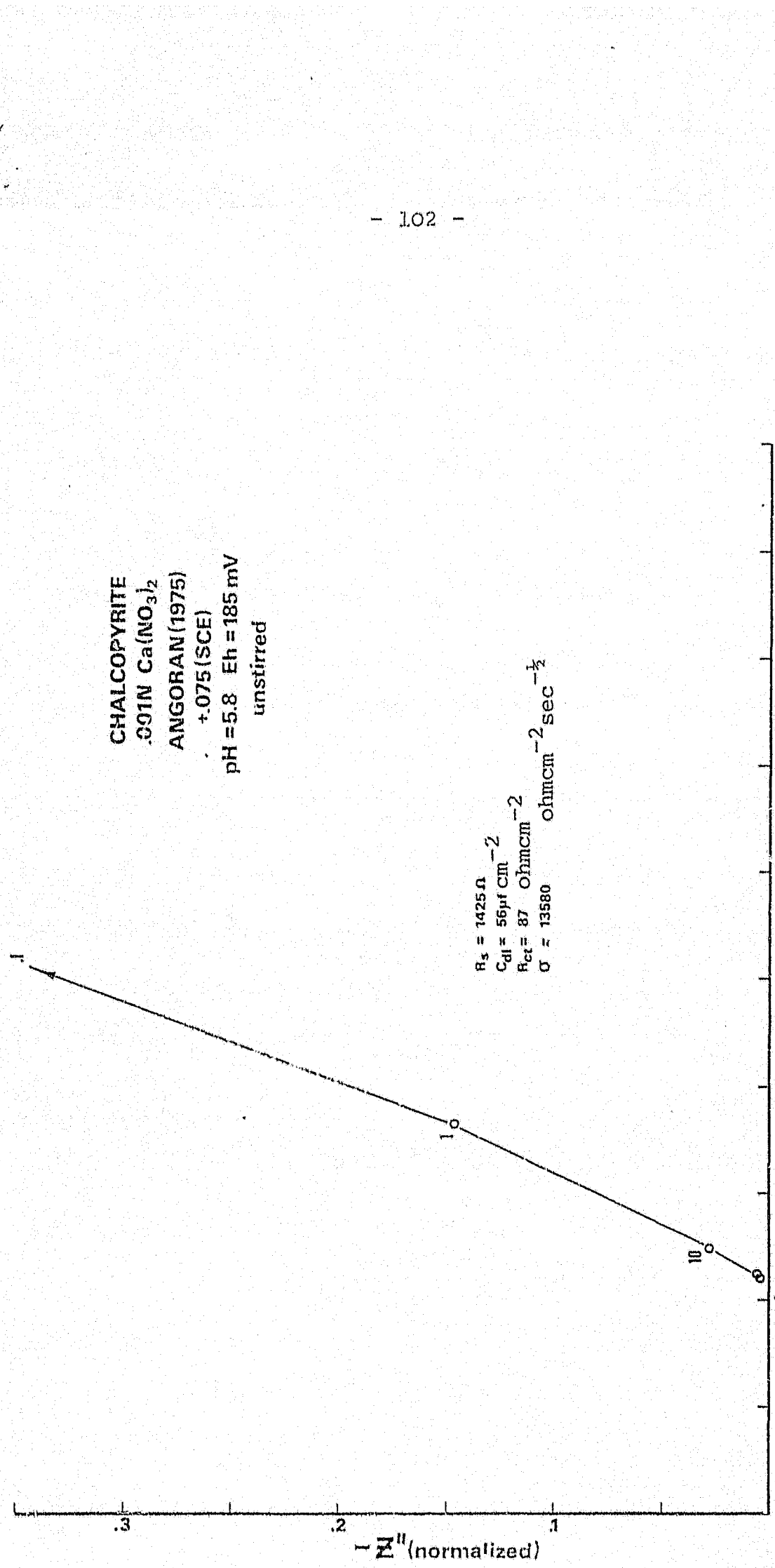

Fig. 4.25. Complex plane plot of chalcopyrite impedances measured by Angoran (1975).

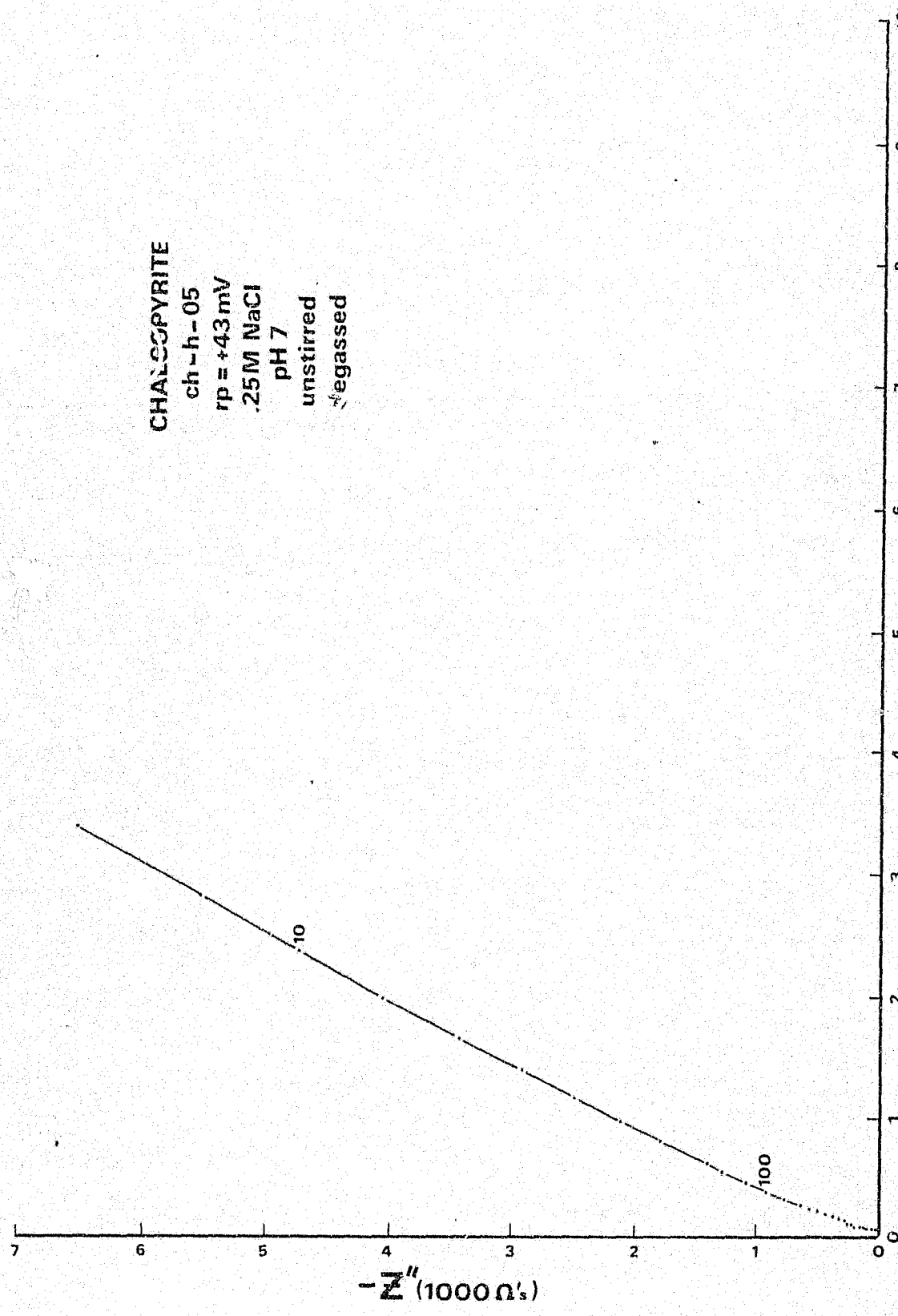

Fig. 4.26. Complex plane plot of rest potential impedance spectrum for chalcopyrite. Note expanded scale.

a depolarizer and using more anodic potentials, some very exotic spectra resulted. The spectra are presented in Fig. 4.27 for anodic potentials of +400 to +650 mV. The spectra for rest potential up to +400 mV overlayed one another with the only difference being the location of particular frequencies along the spectra. Only beyond +500 mV did significant divergence appear. The spectra from +550 to +650 mV have an inductive loop that, for +650 mV, actually recrosses the higher frequency portion of the spectrum. This is interesting in that more than one frequency is associated with an identical impedance, which eliminates mathematical uniqueness. This simple fact tremendously complicates the theory necessary to describe the interface. Other researchers have observed inductive effects but none have properly defined the source or cause of the phenomena involved. The spectra are presented in this research as an oddity and also as a reminder that the ultimate model for sulfide behavior will not be a simple one.

The locus of the 10 Hz values approximately describes a semicircle with the centre near the ordinate. This indicates that the 10 Hz and higher frequencies conform nicely to a simple charge transfer model and that whatever produces the inductive phenomenon is relatively ineffectual above 10 Hz. It should also be noted that the charge transfer semicircle does not appear at anodic potentials lower than +400 mV but rather the 10 Hz values, and all other frequencies, slide up the spectrum. This indicates an increase in overall impedance but no change in rate limiting process.

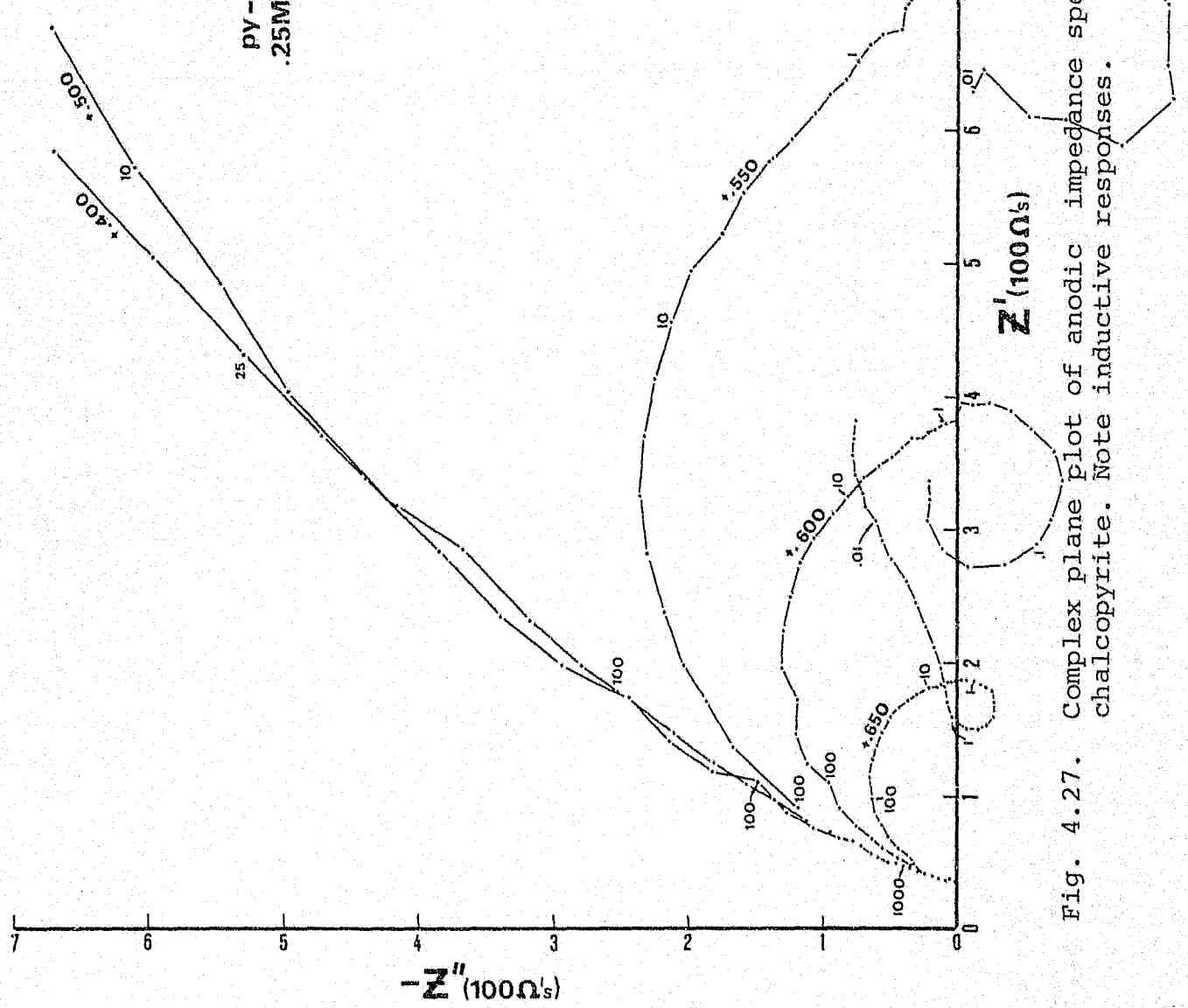

Fig. 4.27. Complex plane plot of anodic impedance spectra for pyrite and chalcopyrite. Note inductive responses.

4.6.4 Chalcocite

An impedance spectrum for chalcocite at a rest potential of +23 mV is shown in Fig. 4.28. As with pyrite and chalcopyrite, chalcocite impedance appears to show a predominantly charge transfer reaction rate limiting process with a tendency towards diffusion control at lower frequencies. An estimated R_{ct} is 43 000 ohms but is questionable due to the probable diffusional interference. The centre of the best fit semicircle lies below the abscissa on an angle of 18.5^{o}. R_s is measured to be approximately 38 ohms.

However, when slightly anodic potentials are applied, chalcocite rapidly begins dissolving and going into solution. This is quite evident in the impedance shown in Fig. 4.29. The spectrum for +100 mV clearly shows a solution Warburg impedance due to the copper chloride diffusing into the solution. It is also noted that the charge transfer reaction semicircle has shrunken considerably and is just discernible. This further suggests a smaller initial R_{ct}. As would be predicted, with a further increase in anodic potential to +200 mV the transition between charge transfer control and diffusion becomes quite obvious. With another 100 mV anodic step in potential the spectrum is considerably reduced in size but the interaction of the ac diffusion layer with the Nernstian diffusion layer produces an interesting circular arc at low frequencies preceded by a 45^{o} solution Warburg slope. Yet another 100 mV anodic step to +500 mV reduces the entire spectrum to a scatter of points around 38 ohms. At this potential, the electrode was possibly dissolving and the solution getting quite murky. The impedance, under these

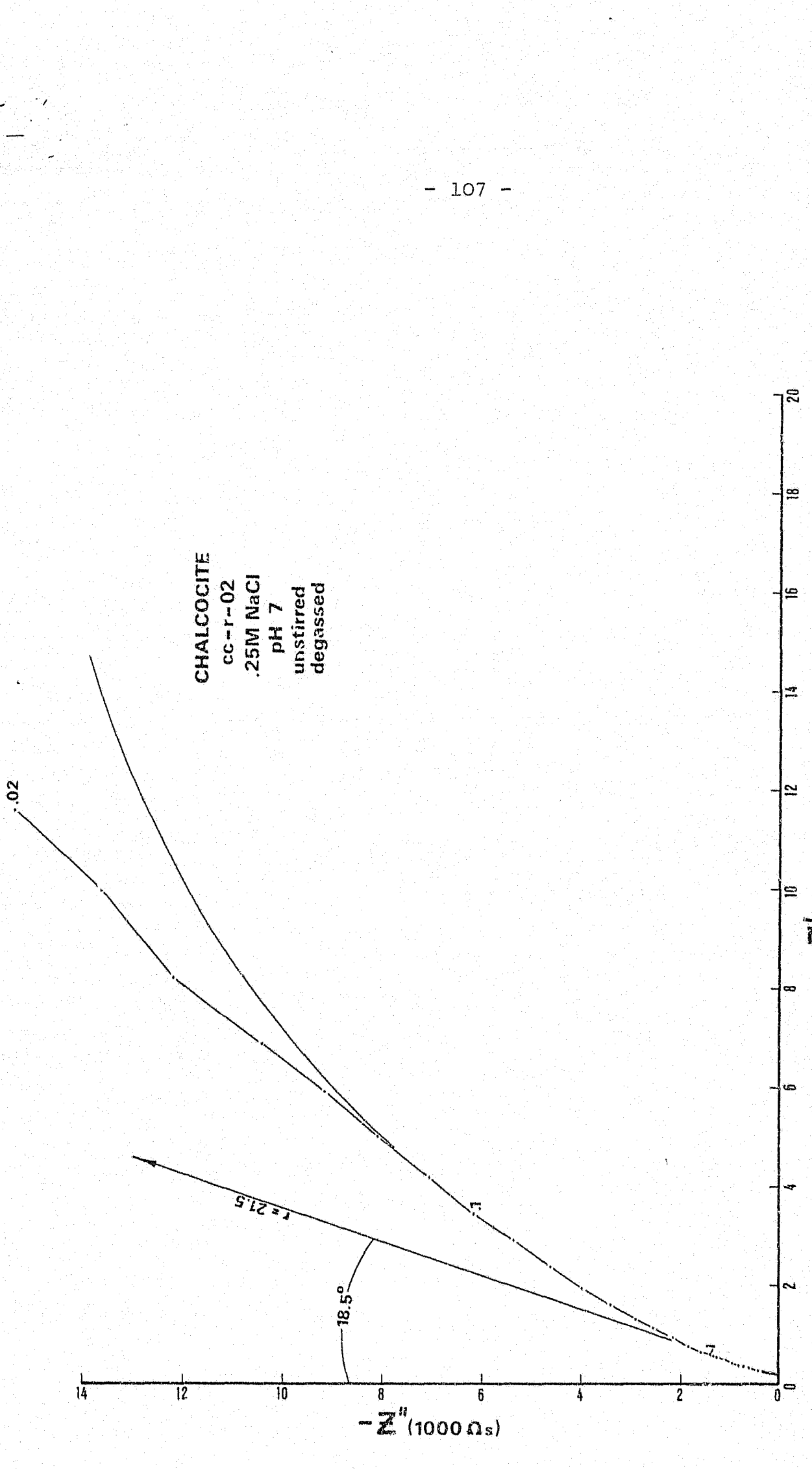

Fig. 4.28. Complex plane plot of a rest potential impedance spectrum for chalcocite.

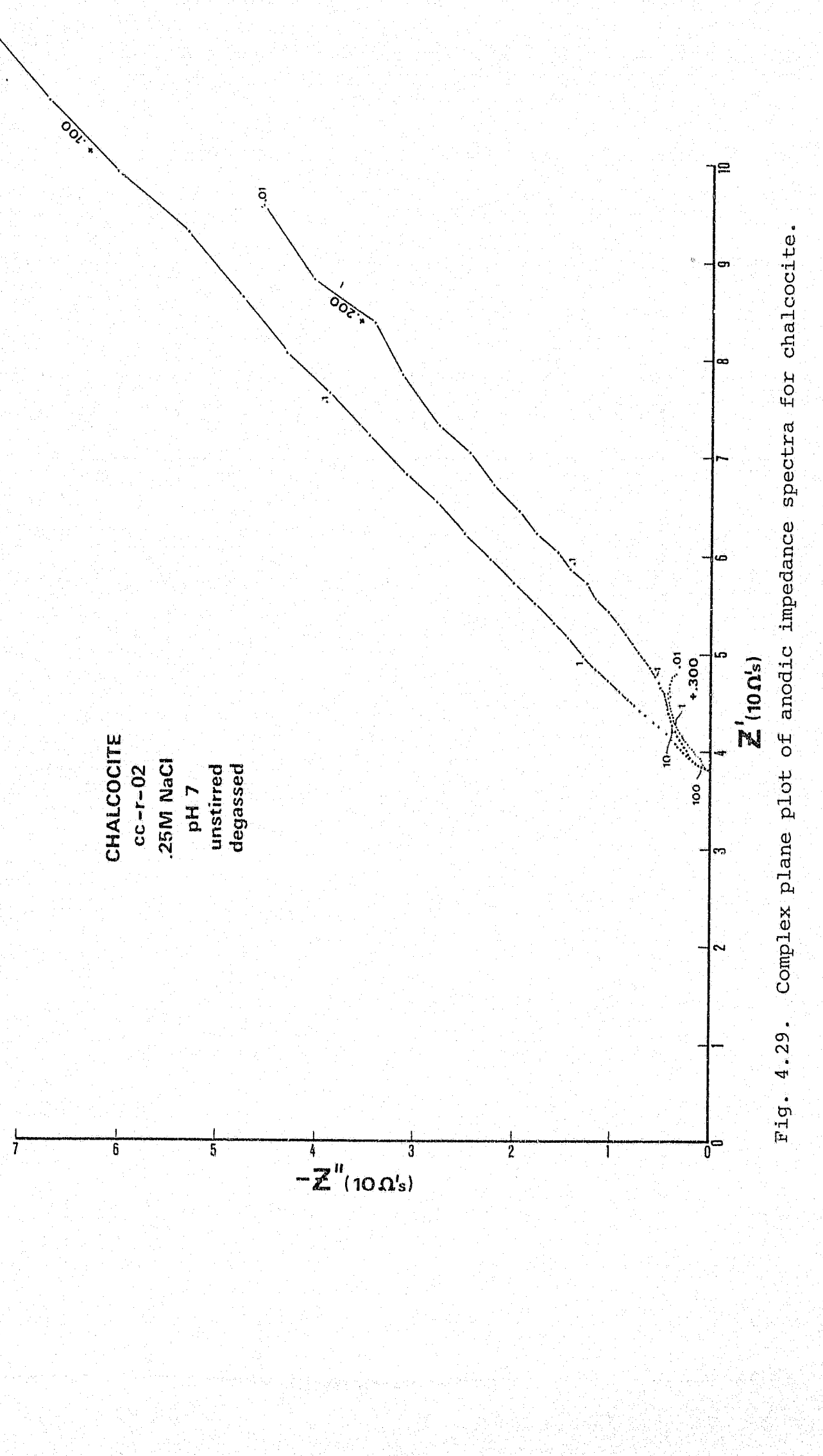

Fig. 4.29. Complex plane plot of anodic impedance spectra for chalcocite.

circumstances, reduces to a simple resistance.

Chalcocite was obviously the most cooperative electrode material in that it behaved very predictably and obeyed the basic principles described earlier.

4.7 Summary

The data presented in this section are the results of consolidating data. More data have been collected than are presented, but if included, would add little to the interpretation. The salient features of the impedance measurements are: 1. charge transfer plays major role in determining the observed impedance at an interface, 2. solution Warburg impedance appears to play a minor role in determining the interfacial impedance, 3. a solid state or surface diffusion impedance may be necessary to describe certain effects seen in the spectra, and 4. individual sulfides and combinations of sulfides will require a complex equivalent circuit to represent the interfacial impedance.

The effectiveness of the method of complex plane analysis should be apparent. A few simple models combined with an adequate amount of data can quickly result in a qualitative and quantitative interpretation of important interfacial parameters. Computer modeling can and should be saved until a representative equivalent circuit can be qualitatively determined through complex plane analysis.

5 CONCLUSIONS

5.1 General

Voltammetric and impedance measurements have been made on some naturally occurring base metal sulfides. These measurements were performed for the explicit reason of determining whether or not individual sulfide types have readily observable and diagnostic electrochemical characteristics. This research is, at best, another step towards a better understanding of the IP phenomenon and was not intended to be definitive. Certainly, the results obtained from this research are limited by the electrochemical cell parameters that were employed. These limitations must be kept in mind whenever the interpretations are extended beyond the controlled situation which itself is artificial and far different from in situ conditions encountered by the sulfides. Nevertheless, the results are very encouraging and make it painfully clear that a great deal more research is necessary. The present research was performed in a logical sequence utilizing gradually more complex electrochemical techniques to build a sound basis for the next technique. This approach has not been used previously and has been very rewarding. So much so, in fact, it is strongly recommmended that future researchers in this field adhere to it as closely as possible.

5.2 Results

The current-voltage curves show definite differences between the sulfide types tested. However, the main purpose of performing current-voltage measurements was to determine the potential limits of minimal current flow, i.e. the range of stability in the current-voltage plane. In these stability ranges the impedance measurements were made. Significant differences observed in the current-voltage curves exist only beyond the stability range, and influence the stability range only by delimiting it. Consequently, in using IP techniques, these differences would not normally be observed. They do have an application however, in that in situ current-voltage measurements may be made, as described by Ryss (1971) and Klein (1977).

By definition, the net current flow in the stability range is either zero or very nearly zero. The stability range is also linear. The gradient of the stability range is very small indicating that (under potentiostatic control) a large change in potential (within the stability range limitations) creates a rather small change in current. Conversely, a small change in current (under galvanostatic control) creates a large change in potential. This latter approach is that of the IP method. In fact, it is the low gradient of the stability range that makes IP a useable tool. Were the gradients much steeper, the small current densities involved in field techniques would not produce a potential signal of measurable amplitide. Bearing this in mind, it is easy to conceive of a strong reducing or oxidizing environment where conventional IP methods would fail to work. Under normal

circumstances, i.e. slightly oxidizing or reducing environments, the stability range is of sufficiently low gradient to produce the desired signal. IP definitelyworks and has been substantiated by countless geophysical surveys. However, this ohmic stability range is not the only determining factor involved in IP. It is only the background against which the time dependent or impedance phenomena are observed. These phenomena can only be studied by dynamic techniques such as cyclic voltammetry or special methods.

The impedance measurements made in the stability ranges showed distinct differences between sulfides of differing composition. When making the impedance measurements, a problem arose in trying to demonstrate the solution diffusion Warburg impedance. After repeated unsuccessful attempts, it became apparent that solution diffusion was not a major contributor to the observed impedance of some sulfides as has been propounded by Madden et al (1957-1959) and Angoran (1975). This observation is considered to be the major contribution of this research.

As previously mentioned, Zonge (1972) and Katsube and Collett (1973) have observed differences in impedance spectra that were attributed to sulfide types. For such discrimination to be possible implies sulfide dependent rate limiting mechanism. This is contrary to a solution dependent rate limiting mechanism. Therefore, the implication of the present research is that: 1. sulfide dependent rate limiting mechanisms do exist, 2. they dominate solution rate limiting mechanisms for certain sulfides, and 3. they

are observable in impedance spectra.

With the appearance of what appear to be contradictory results to ideas currently in vogue, one is provoked by the immediately obvious questions: Are the data valid?, Were the proper approaches used?, Were the interpretations justified?, and, if these can be answered in the affirmative.....Whom is correct?

5.2.1 Are the data valid?

Data qualities are relative when comparing one data set to another, and clearly depend on the results to be achieved from using the data. In the current case there are effectively three comparable data sets: 1. that of Madden and Marshall (1959), 2. that of Angoran (1975), and 3. that of the present research. Fortunately having only three sets facilitates comparison.

5.2.1.1 Data of Madden and Marshall

The data of Madden and Marshall were collected in the late 1950's using state of the art electronics. They used a bridge balancing approach and measured phase shifts by observing Lissajous figures on a CRO. This is an accurate method for making impedance measurements especially at frequencies greater than 10 Hz, and in no way would invalidate their data. Phase errors may have existed at frequencies less than 10 Hz, but were a minor problem considering the dynamic range involved. They measured phase and magnitude at half decade intervals from .01 to 1000 Hz with an overall accuracy of about $\pm$ 5% (p.47). This results in ten data points per spectrum. No problems with data validity are

apparent.

5.2.1.2 Data of Angoran

Instrumentally, Angoran followed in the footsteps of Madden et al, and also used a bridge balancing technique for magnitude and measured phase shifts by observing Lissajous figures on a CRO. Newer equipment was used but the relative phase errors at low frequencies would have been about the same as Madden et al. Still, this would not invalidate the data. Only decade impedance measurements were made over the same frequency range resulting in only five data points per spectrum. Considering the comprehensive effort made by Angoran, it is difficult to slight this one aspect of the data collection. However, this minimum number of data points has certain limitations that will be discussed under approaches. No problem with data validity are apparent.

5.2.1.3 Present research data

The data presented herein differed from those of Madden et al and Angoran in two distinct ways: 1. the data were collected using an instrument specifically designed for this application which employed a realtime digital correlation technique, and 2. ten data points per decade were measured. The ten points per decade virtually guaranteed good resolution of the spectra. The correlation technique, for a large number of cycles, could produce data accurate to $\pm$ 0.01% for magnitude and $\pm$ 0.1% for phase, although this level of accuracy was considered unnecessary for the gross phenomena desired. Data were gathered from 0.01 to 5000 Hz and resulted in approximately 60 points per spectrum.

Consequently, it would not appear that data validity would contribute to an explanation of the observed differences.

5.2.2 Were the proper approaches used?

How the data are calculated, plotted and interpreted constitutes the approach. The calculation and plotting of data are difficult to take issue with as in all cases the techniques are sound. However, subtle differences observed through different plotting techniques can affect how the data are interpreted.

5.2.2.1 Approach of Madden and Marshall

Madden and Marshall plotted their data using Bode plots, the conventional approach to circuit analysis that is still prevalent today. They took an equivalent circuit (Madden and Marshall, 1959, p.47) and fitted the circuit to the data. The resultant circuit parameters were then compared and the interpretation made from the results of the comparisons. This is a standard approach and is only limited by the choice of the equivalent circuit. As the circuit used is fairly comprehensive, it should cover most rate limiting processes likely to be encountered. No fault can be found with this aspect of their research.

5.2.2.2 Approach of Angoran

The approach of Angoran is very similar to that of Madden and Marshall. Minor exceptions are that Angoran did not make Bode plots but rather plotted the value of the fitted circuit Warburg impedance in Pourbaix diagrams as a function

of Eh and pH. Angoran evidently started with the equivalent circuit of Madden and Marshall but "came to the inexorable conclusion" that a Randle's circuit would suffice. Only the fitted data for the latter were presented. The earlier circuits allowed for a surface Warburg impedance and a good discussion is given to the topic. However, one can only assume that the surface Warburg coefficient was quite small relative to obscurity by later exclusion from the circuit. When considering the approach used, i.e. fitting circuits with and without certain elements, it is not surprising that most of the earlier second order elements were discarded. It would seem that a simple test to observe the effects of these circuit elements would supply better criteria for evaluation e.g. stirring and nonstirring to evaluate solution diffusion. The lack of supporting tests and the fact that only five data points are available per spectrum suggest a definite weakness in the approach.

5.2.2.3 Approach of present research

The approach of the present research, as previously discussed, was to perform an adequate suite of electrochemical measurements so that single hypotheses might have support by more than one technique. Through using a higher density of data in the impedance measurements and plotting the data in the complex plane the effects of the primary interfacial parameters were very pronounced. By qualitative comparison with a suite of theoretical curves derived from increasingly complex equivalent circuits (but not as complex as that of Madden and Marshall or Angoran), the rate con-

trolling processes were readily determined. Since the measuring apparatus presented the reduced data in the complex plane it was easy to judge and test the circuit parameters. In so doing, it was determined that with pyrite and chalcopyrite solution diffusion was virtually unobservable. Angoran's data were plotted and compared with the present data. In the complex plane, the poor definition due to the lack of data became evident. Nevertheless, the data, if reinterpreted, fitted the non-solution diffusional model indicated by this research. But conversely, due to stirring tests, the present data could not be fitted by a circuit using only solution diffusion.

It is in the approach and interpretation that the significant differences occur.

5.2.3 Were the interpretations justified?

Within the limitations of the three research efforts involved it would be difficult to say that any one interpretation was not justified. It is only because of the particular approach used that a difference in interpretation exists at all. Each researcher adequately established the framework within which he was working. This, in turn, defined the limitations of the interpretations.

5.2.4 Whom is correct?

The ultimate question. For the reasons cited, I feel the present research has a high enough degree of validity to justify the statements made and to warrant serious consideration. The presently accepted views of the primary rate limiting mechanism controlling the IP phenomonon being that

of solution diffusion are suspect. It is felt that the surface diffusion is the phenomonon observed when the charge transfer reaction becomes subordinate. The research effort of Madden and Marshall, and Angoran produced similar data but through a different approach arrived at different conclusions regards solution and surface diffusion. Consequently, the possibility of sulfide discrimination was dismissed as highly unlikely. If, for no other reason than to invalidate the present research, someone else investigates the diffusion question and arrives at an unequivocal answer, this research has served its purpose. Should solution diffusion ultimately prove to play a minor role and surface diffusion a major role, in determining the interfacial impedance then the possibility of sulfide discrimination will become a certainty as surface diffusion is an intrinsic property of a solid.

5.3 Epilogue

The conclusions presented in this research should not be considered final but hopefully will be tested further and used toward reorienting future research in this area to include diagnostic electrochemical tests. The thrust of the present research was not to test purely the diffusional aspects of the interfacial phenomena but to observe general interfacial parametric relationships. This was accomplished but the solution diffusion issue clearly permeates the effort.

APPENDIX A. ELECTRODE PREPARATION

A.1 Electrode Design

The electrodes used in this research were fabricated by hand from naturally occurring sulfide minerals. The design is similar to that of commercially available ion selective electrodes marketed by Van Waters and Rogers Scientific Division of Univar (1976 catalogue, p.934). A schematic cross-sectional view is shown in Fig.A.1.

The process of making the electrodes was the most time consuming aspect of the research. A variety of electrode designs and fabrication techniques were attempted and tested but the design chosen was preferred because of ease of surface preparation, ease of sulfide-resin casting and overall flexibility in use. A total of 111 useable electrodes were made.

A.2 Sample Selection and Sizing

The ideal electrodes for this type of work should be composed of pure material containing no structural defects. Since such high quality material is not available in the desired size range, naturally occurring sulfides that best approximated these criteria were selected. In most instances impurities were not visible and structural defects were avoided, when possible. No analyses were performed on the samples. Where major flaws or inclusions were present they were covered or impregnated with wax or epoxy resin during

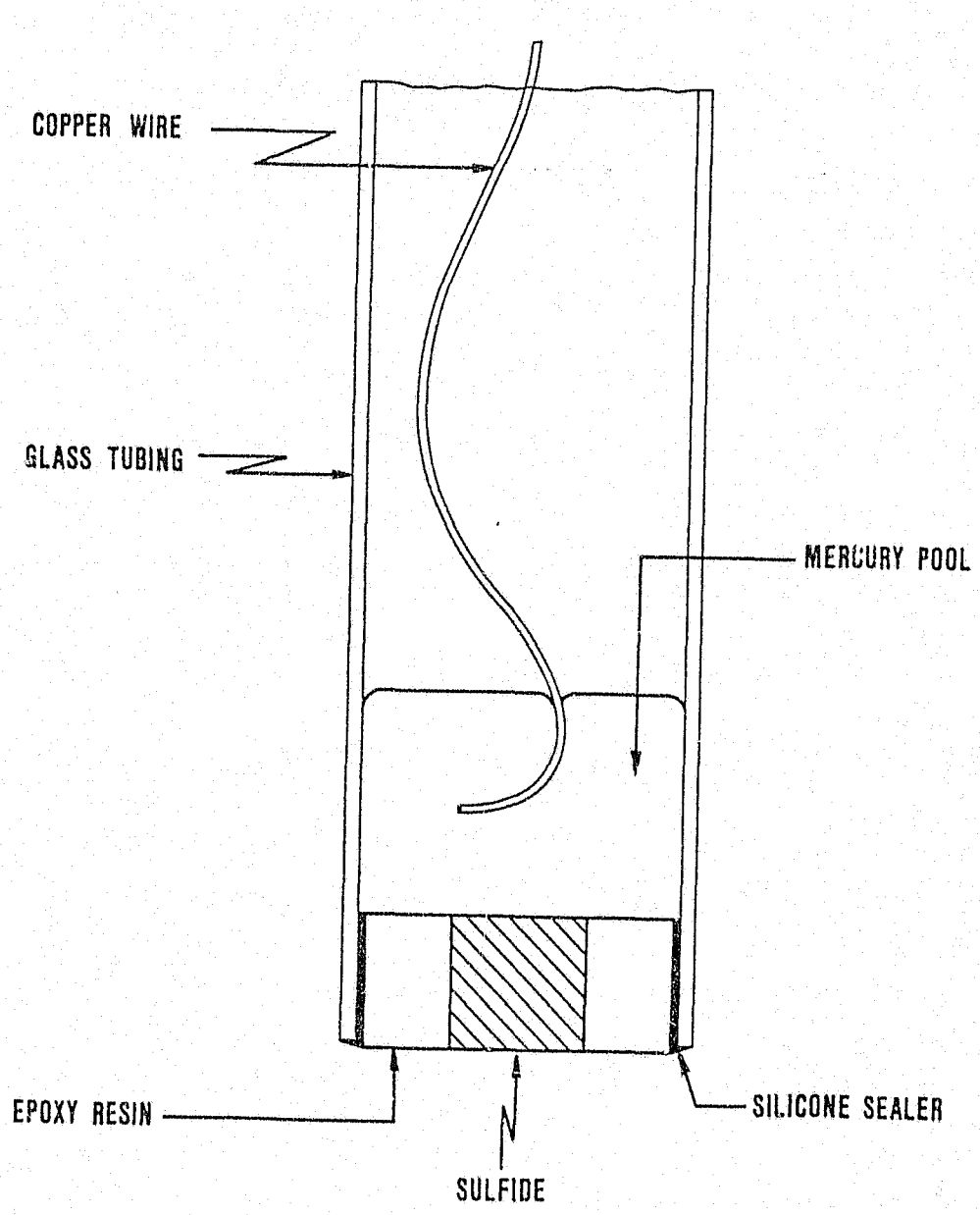

Fig. A.1. Schematic cross-sectional view of a typical electrode used in this research.

the mounting stage.

The samples were first crudely sized simply by breaking them into useable dimensions. A sample about five mm in diameter and about ten mm long was considered optimal. These samples were then hand held and ground into crude cylindrical shape (as were the fingers).

A.3 Casting

After grinding, all samples were ultrasonically cleaned in metal-free water. Supporting wires were then bonded to one end of each sample. The wire was used to locate and support the sulfide in the casting stage. The samples were cast in Standard Brands Casting Resin in molds made of glass tubing, apporximately 75 mm long with one sealed end. The casting process consisted of first partially filling the tubing with resin, coating the sample with resin, and then slowly inserting the sample into the resin in the tubing. Avoiding sample contact with the sides of the tubing was essential in order to eliminate sealing problems later. The samples and resin were then placed in a bell jar and held under partial vacuum for approximately one minute. This step removed air from the samples. When the partial vacuum was released, the resin was forced into the holes in the samples. The castings were then cured at ambient temperature for one hour, heated to 50^{o}C for 8 hours and slowly cooled. All casting was done under a ventilation hood to avoid the spoxy resin fumes.

A.4 Sawing and Sealing

The sealed ends were then sawed off and the casting pushed

out of the tubing. The portion of the casting containing the sample was then sawed into as many 5 mm thick wafers as sample dimensions allowed, using a 0.040 mm thick diamond saw with a specially built jig. All samples were again ultrasonically cleaned. The surfaces were then microscopically inspected and the best surface of each wafer marked for polishing.

Seebeck thermoelectric semiconductor carrier type tests were performed at this stage. The results are presented in Appendix B.

Each wafer was then inserted into the end of a 100 mm long piece of 12 mm glass tubing using Dow Corning Silicone Rubber Sealer No. 684. Soft curing sealer allowed for reuse of the wafers in the event of tubing breakage. The tubing and wafers were cleaned with acetone immediately prior to the application of sealer to improve the sealer bond. A vee-shaped jig was made to enable proper alignment of the wafer and tubing. This assembly stage was performed under a microscope and all unnecessary sealer was carefully trimmed off with a razor blade. The sealer provided a water tight seal at a pressure of a least 100 mm of water and was electroactively inert. The wafers were left protruding about one mm beyond the end of the tubing to enable polishing prior to and after usage. Since this end of the electrode was to be immersed in electrolyte and a constant surface area was necessary, any exposed sulfide other than the normal surface was covered with sealer.

A.5 Polishing

The final stage in preparation was polishing and was performed in five steps using a cylindrical PVC jig to maintain the proper orientation of the electrodes. First pass polishing was done on 240 grit paper to true the surface and eliminate saw marks. The second through fifth steps used progressively finer grits; 600, 1000, 9 micron and 1 micron, respectively. The polishing stage completed the normal preparation but most electrodes had holes or cracks in the surface requiring filling with epoxy resin and re-polishing.

A.6 Wax Impregnation

A select number of electrodes and adequate wax pellets were placed in a heavy wall, filtering, Erlenmeyer flask. The flask was then heated until the wax melted and covered the ends of the electrodes. The temperature was maintained at a low enough value to keep the wax fluid but not endanger the sulfides. The flask was evacuated to 5 mm of mercury for 15 minutes, brought to 1 bar with dry nitrogen and held for one minute. This procedure was repeated (using 3 minutes instead of 15) until no more bubbles were evident. The electrodes were then removed and wiped with tissues.

A.7 Surface Area Determination

Once the electrodes were completed, the sulfide ends were microphotographed and the projected surface area was determined using both a scanning densitometer and a planimeter

on the phctographs. At best, the surface area measurements are approximate due to the intrinsically rough and porous nature of the sulfide material, though it was hoped that resin and wax impregnation minimized the problem.

A.8 Ohmic Contact

Ohmic contact to the sulfide particle was achieved by placing approximately 10 mm of mercury on top of the sulfide wafer inside the tubing. Acopper wire was inserted into the mercury but not allowed to make contact with the sulfide sample. The resultant current path in the electrode was from the sulfide, through the mecury to the copper wire. Each material is an electronic conductor and is of low resistance. The mercury acts neither as an injector nor collector of minority carriers (Donovan and Reichenbaum, 1958) and provides a non-rectifying, or ohmic, contact.

B. SEMICONDUCTIVITY DETERMINATIONS

B.1 Seebeck Thermoelectric Effects

When a thermal gradient is applied to a material and an observable electric current is produced, the phenomenon is called the Seebeck effect. Seebeck measurements were made on the electrode samples using the facilities of the Dept. of Electrical Engineering at the University of Arizona.

According to Telkes (1950) and Shuey (1975), the semiconductor type (p or n) is defined and determined by the voltage gradient relative to the thermal gradient. When the thermal gradient is positive and the voltage gradient negative, the charge carriers are p-type. When both the thermal and voltage gradients are positive, the charge carriers are n-type.

B.2 Purpose

The samples were tested for semiconductivity type prior to mounting in the glass holders so as to have the information in hand should there by any noticeable correlation with electrochemical responses. None were observed.

B.3 Results

The results are presented in Table B.1. All results are in agreement with those reported by Shuey (1975).

TABLE B.1.

THERMOELECTRIC (SEEBECK) DETERMINATION OF CARRIER TYPE

Mineral	Location	ID	Quantity	Carrier type
pyrite	Washington Camp, Mowry, Ariz.	(w)	6	n
pyrite	Alice Mine, Idaho Spgs, Colo.	(a)	11	n
pyrite	Ambassaguas, Spain	(s)	3	n & p
pyrite	Balmat, New York	(d)	5	n
pyrite	Balmat, New York	(b)	1	n & p
pyrite	Trabzon, Turkey	(t)	2	n
pyrite	Unknown (EDM)*	(u)	2	n & p
marcasite	Unknown	(u)	6	p
pyrrhotite	Santa Eulalia, Mex.	(e)	11	n
pyrrhotite	Horne Mine, Quebec Canada	(h)	4	n
chalcopyrite	Horne Mine, Quebec Canada	(h)	12	n
chalcopyrite	Kidd Creek, Ont. Canada	(k)	5	n
chalcopyrite	Mission Mine, Tucson, Ariz.	(m)	6	n
chalcopyrite	Unknown	(u)	3	n
bornite and chalcocite	Magma Mine, Superior, Ariz.	(m)	7	p
chalcocite	New Cornelia Mine Ajo, Ariz.	(a)	10	p
chalcocite	Ray Mine, Ray, Ariz	(r)	9	p
chalcocite	San Juan Mine, Safford, Ariz.	(s)	10	p

*Electro-discharged machined

TABLE B.1.

THERMOELECTRIC (SEEBECK) DETERMINATION OF CARRIER TYPE

Mineral	Location	ID	Quantity	Carrier type
pyrite	Washington Camp, Mowry, Ariz.	(w)	6	n
pyrite	Alice Mine, Idaho Spgs,Colo.	(a)	11	n
pyrite	Ambassaguas, Spain	(s)	3	n & p
pyrite	Balmat, New York	(d)	5	n
pyrite	Balmat, New York	(b)	1	n & p
pyrite	Trabzon, Turkey	(t)	2	n
pyrite	Unknown (EDM)*	(u)	2	n & p
marcasite	Unknown	(u)	6	p
pyrrhotite	Santa Eulalia,Mex.	(e)	11	n
pyrrhotite	Horne Mine, Quebec Canada	(h)	4	n
chalcopyrite	Horne Mine, Quebec Canada	(h)	12	n
chalcopyrite	Kidd Creek, Ont. Canada	(k)	5	n
chalcopyrite	Mission Mine, Tucson, Ariz.	(m)	6	n
chalcopyrite	Unknown	(u)	3	n
bornite and chalcocite	Magma Mine, Superior,Ariz.	(m)	7	p
chalcocite	New Cornelia Mine Ajo, Ariz.	(a)	10	p
chalcocite	Ray Mine, Ray,Ariz	(r)	9	p
chalcocite	San Juan Mine, Safford, Ariz.	(s)	10	p

*Electro-discharged machined

Appendix C REFERENCE ELECTRODES

C.1 Three Requirements

The three main requirements for a satisfactory reference electrode are: 1. reversibility, 2. reproducibility, and 3. stability, which are all interrelated quantities (Janz and Ives, 1968).

The quantitative measure of the first of these is the exchange current. Unless a reference electrode has a high exchange current, its potential will depart from its equilibrium value when current demands are made on it.

Reproducibility covers two aspects; the ability of a particular electrode specimen to respond according to the Nernst equation without temperature (or concentration) change hysteresis, and the feasibility of establishing a standard method of electrode preparation, which will produce electrodes on one or many occasions that group acceptably about a mean potential, i.e. show small bias potentials.

The third requirement, stability, is self explanatory, referring also to the useful life of an electrode system. How closely it is necessary to satisfy these three basic requirements depends on the use to which the reference electrode is put (Covington, 1968).

C.2 Calomel Electrode

Too often, reference electrodes are selected on their availability or ease of construction and their inherent limitations are overlooked. The primary function of the reference electrode in regards to the present investigations is that of (ideally) invariant potential. For this research, a saturated or 3.5M KCl calomel electrode (SCE) was used. An additional polyacrylamide salt bridge with frit is employed to minimize contamination from the use of a variety of electrolytes.

C.3 Limitations

As a potential invariant electrode, the calomel electrode has distinct limitations, principally due to temperature hysteresis effects which are the results of disproportionation of calomel (Hills and Ives, 1961). Other shortcomings are sensitivity to oxygen and time dependency of the potential immediately after manufacture. These effects were overcome by letting the electrode stabilize for over six months. Temperature effects were ignored as all experiments were performed at or near constant temperature and pressure.

C.4 Half-cell Potential

The procedure for determining the half-cell potential (Pecsok and Shields,1968) is as follows. The half-cell is designated by:

$$Hg \left| Hg_2Cl_2, KCl(sat) \right. \qquad C.1$$

C.2 Calomel Electrode

Too often, reference electrodes are selected on their availability or ease of construction and their inherent limitations are overlooked. The primary function of the reference electrode in regards to the present investigations is that of (ideally) invariant potential. For this research, a saturated or 3.5M KCl calomel electrode (SCE) was used. An additional polyacrylamide salt bridge with frit is employed to minimize contamination from the use of a variety of electrolytes.

C.3 Limitations

As a potential invariant electrode, the calomel electrode has distinct limitations, principally due to temperature hysteresis effects which are the results of disproportionation of calomel (Hills and Ives, 1961). Other shortcomings are sensitivity to oxygen and time dependency of the potential immediately after manufacture. These effects were overcome by letting the electrode stabilize for over six months. Temperature effects were ignored as all experiments were performed at or near constant temperature and pressure.

C.4 Half-cell Potential

The procedure for determining the half-cell potential (Pecsok and Shields,1968) is as follows. The half-cell is designated by:

$$Hg \left| Hg_2Cl_2, KCl(sat) \right. \qquad C.1$$

The potential can be derived from the primary reaction:

$$Hg_2^{++} + 2e^- = 2Hg \qquad C.2$$

and the corresponding Nernst equation:

$$E = E^0_{Hg} - \frac{0.059}{2}\log\frac{1}{Hg_2^{++}} \qquad C.3$$

The concentration of Hg_2^{++} is controlled by the concentration of Cl^- which is essentially the same as the solubility of KCl. Chloride ion from Hg_2Cl_2 is negligible compared to that from KCl. Therefore,

$$E = E^0_{Hg} - \frac{0.059}{2}\log\frac{(Cl^-)^2}{K_{Hg_2Cl_2}} \qquad C.4$$

where $K_{Hg_2Cl_2}$ is the solubility product of Hg_2Cl_2

Rearranging the equation, a new E^o term can be defined:

$$E = E^0_{Hg} + \frac{0.059}{2}\log K_{Hg_2Cl_2} - 0.059\log(Cl^-) = +0.242 \qquad C.5$$

Because the potential is controlled by a species that does not take part in the electrode reaction, this is known as an electrode of the second order or anion reversible.

APPENDIX D. CELL DESIGN

D.1 Cell Geometry

Cell geometry is probably the most important factor in cell design. The nature of the proposed studies also strongly influences electrode placement within the cell. It is desirable that the electrodes be symmetrically placed to minimize potential gradients at the working electrode arising from different iR drops through variation in the electrolyte path between the working and auxiliary electrodes. The arrangement used for the voltammetric measurements was that of a planar electrode located axially orthogonal within a cylindrical gauze type platinum mesh. This was at best a compromise between other designs, available equipment and physical limitations of the working electrode materials.

D.2 Luggin Capillary

The most immediately obvious shortcoming of this arrangement is that current paths are of various lengths creating higher current densities near the edges of the working electrode. This circumstance can be taken advantage of by placing the Luggin capillary (LC) near the centroid of the working electrode surface where the potential gradients should be the least. This optimizes the repeatability of the iR drop between the LC and the working electrode (WE) due to location errors by avoiding the high potential gradients near the edges. That such gradients exist on

working electrodes can be demonstrated by making an equipotential map of the electrolyte. A variety of tip designs for the LC have been classified according to the direction of approach to the WE and the type of tip opening. For the present research a frontal approach using an open and remote tip form was considered adequate and most expedient. A certain amount of screening effect is created in a frontal approach but is virtually impossible to eliminate.

A noticeable stress is put on the location of the LC as generally small errors in potential measurement can be tolerated in most investigations but serious problems arise in pulsed or square wave techniques. When the cell is subjected to a step function the WE response reflects the conditions at the electrode/electrolyte interface. Initially there is no faradaic current passed until the double layer is charged. Thereafter, the rate of reaction is determined by the value of the faradaic current. At low overpotentials the faradaic current is directly proportional to the overpotential but the relationship follows the exponential Tafel law at larger overpotentials. Consequently, at appreciable faradaic currents, the iR error introduced by the resistance of the electrolyte between the LC and the WE may markedly influence the actual potential produced at the WE. This can lead to invalid interpretation of the kinetic reactions since the current-overpotential relationship is altered and the actual reaction mechanism modified.

D.3 Impedance Cell

A slight modification for the impedance measurements was

BIBLIOGRAPHY

Adams, R.N., Electrochemistry At Solid Electrodes, New York, Marcel Dekker, Inc., 1969.

Angoran, Y.E., 'Induced Polarization of Metallic Minerals, A Study of Its Chemical Basis', Ph.D. Thesis, M.I.T., 1975.

Angoran, Y.E., and Madden, T.R., 'Induced Polarization: A Preliminary Study of Its Chemical Basis', Geophysics, 42:788-803, 1967.

Armstrong, R.D., and Bell, M.F., and Metcalfe, A.A., 'An Introduction to Chemical Impedance Analysis', Electrochemistry Research Laboratory, University of Newcastle Upon Tyne, 1976.

Bockris, J.O'M., and Reddy, A.K.N., Modern Electrochemistry and Physics, New York, Plenum Press, 1973.

Covington, A.K., 'Ion Selective Electrodes', National Bureau of Standards Special Publications 314, Wash. D.C., 1969.

Delahay, P., New Instrumental Methods in Electrochemistry, New York, Interscience Pub. Co., 1954.

DeRosa, J.F., and Beard, R.B., 'Linear AC Electrode Polarization Impedance at Smooth Noble Metal Interfaces', IEEE Transaction on Biomedical Engineering 24: no. 3, 1977.

Donovan, B., and Reichenbaum, G., 'Electrical Properties of Chalcopyrite', British Journal of Applied Physics, 9:474-477, 1958.

Fisher, W., Personal communication, 1976.

Gileadi, E., and Kirowa-Eisner, E. and Penciner, J., Interfacial Electrochemistry, Ontario, Canada, Addison Wesley Pub. Co., 1975.

Grahame, D.C., 'Mathematical Theory of the Faradaic Admittance', Journal of the Electrochemical Society, 99:370, 1952.

Hansuld, J.A., 'Oxidation Potentials of Pyrite', Ph.D. Thesis, McGill University, Montreal, 1961.

Harvey, R.D., 'Electrical Conductivity and Polished Mineral Surfaces', Economic Geology, 23:778, 1928.

Hills, G.J., and Ives, D.J.G., Reference Electrodes, New York, Academic Press, 1961.

Jahnke, E.L., Tables of Higher Functions, New York, McGraw Hill, 1960.

Janz, G.J., and Ives, D.J.G., Annual of New York Academy of Sciences, 148:210, 1968.

Katsube, T.J., and Collett, L.S., 'Electrical Characteristic Differentiation of Sulphide Minerals by Laboratory Techniques', Paper read at 43rd Annual International Meeting of Society of Exploration Geophysicists, Mexico City, 1973.

Kerr, P.F., and Cabeen, C.K., 'Electrical Conductivity of Ore-Minerals', Economic Geology, 20:, 1925.

Klein, J.D., and Shuey, R.T., 'Nonlinear impedance of mineral electrolyte interface, Part I: Pyrite, and Part II: Galena, Chalcopyrite, and Graphite', Geophysics, 43:1222-1235, 1978.

Lyons, E.H., Introduction to Electrochemistry, Boston, D.C. Heath and Co., 1967.

Madden, T.R., and Marshall, D.J., 'Electrode and Membrane Polarization', Interim Report for U.S. Atomic Energy Commission, Div. of Raw Materials, Contract AT-(05-1)-718, Cambridge, Mass., 1959.

Marinace, J.C., 'Some Electrical Properties of Natural Crystals of Iron Pyrite', Physics Review, 96:, 1954.

Mehl, W. and Hale, J.M., Advances in Electrochemistry and Electrochemical Engineering, 6:399-458, New York, Interscience Pub. Co., 1967.

Myamlin, V.A., and Pleskow, Y.V., Electrochemistry of Semiconductors, New York, Plenum Press, 1967.

Pecsok, R.L., and Shields, D.L., Modern Methods of Chemical Analysis, New York, John Wiley & Sons, Inc. 1968.

Pridmore, D.F., and Shuey, R.T., 'The Electrical Conductivity of Galena, Pyrite, and Chalcopyrite', American Minerologist, 1975.

Randles, J.E.B., 'Kinetics of Rapid Electrode Reactions', Disc. of the Faraday Soc., 1:11-19, 1947.

Ryss, Y.S., 'Contact method of polarization curves', Borehole Mining Geophysics, G.K. Volosyuk and N.I. Safranov, ed., Leningrad, Nedra, 1971.

Sasaki, A., 'On the Electrical Conduction of Pyrite', Mineral Journal, 1:290-302, 1955.

Sato, M., 'Oxidation of Sulphide Ore Bodies, 1. Geochemical Environments in Terms of Eh and Ph', Economic Geology, 55:928-961, 1960.

Shuey, R.T., Semiconducting Ore Minerals, New York, Elsevier Scientific Pub. Co., 1975.

Sluyters, J.H., 'On the Impedance of Galvanic Cells', Rec. Trav. Chim., 79:109-1100, 1960.

Stanton, R.L., 'Studies of Polished Surfaces of Pyrite and Some Implications', Canadian Mineralogist 6: part 1, 1957.

Sumner, J.S., Principles of Induced Polarization for Geophysical Exploration, Amsterdam, Elsevier Scientific Pub. Co., 1976.

Telkes, M., 'Thermoelectric Power and Electrical Resistivity of Minerals', American Mineralogist 35:, 1950.

VanWaters, and Rogers, Scientific Apparatus Catalog, p. 934, 1976.

Vetter, K.J., Electrochemical Kinetics, Theoretical and Experimental Aspects, New York, Academic Press, Inc., 1967.

Zonge, K.L., 'Electrical Properties of Rocks as Applied to Geophysical Prospecting', Ph.D. Thesis, University of Arizona, 1972.